CrystEngComm c3ce41215f

COMMUNICATION

Microwave-hydrothermal synthesis of single-crystalline Co_3O_4 spinel nanocubes

Tatiana A. Mulinari, Felipe A. La Porta,* Juan Andrés, Mário Cilense, José A. Varela and Elson Longo

An efficient microwave-hydrothermal method has been developed for the synthesis of highly crystalline Co_3O_4 spinel nanocubes *via* β-$Co(OH)_2$ without any surfactant assistance.

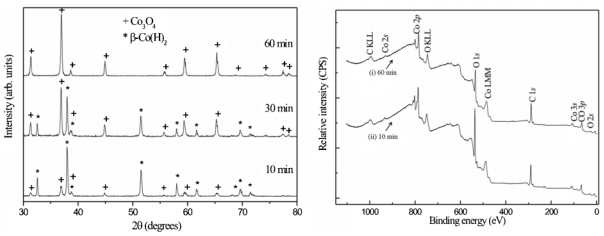

3

Please check this proof carefully. **Our staff will not read it in detail after you have returned it.**

Translation errors between word-processor files and typesetting systems can occur so the whole proof needs to be read. Please pay particular attention to: tabulated material; equations; numerical data; figures and graphics; and references. If you have not already indicated the corresponding author(s) please mark their name(s) with an asterisk. Please e-mail a list of corrections or the PDF with electronic notes attached — do not change the text within the PDF file or send a revised manuscript. Corrections at this stage should be minor and not involve extensive changes. All corrections must be sent at the same time.

Please bear in mind that minor layout improvements, e.g. in line breaking, table widths and graphic placement, are routinely applied to the final version.

We will publish articles on the web as soon as possible after receiving your corrections; **no late corrections will be made.**

Please return your **final** corrections, where possible within **48 hours** of receipt, by e-mail to: crystengcomm@rsc.org

Queries for the attention of the authors

Journal: **CrystEngComm**

Paper: **c3ce41215f**

Title: **Microwave-hydrothermal synthesis of single-crystalline Co_3O_4 spinel nanocubes**

Editor's queries are marked like this... [1], and for your convenience line numbers are indicated like this... 5.

Please ensure that all queries are answered when returning your proof corrections so that publication of your article is not delayed.

Query Reference	Query	Remarks
1	For your information: You can cite this article before you receive notification of the page numbers by using the following format: (authors), CrystEngComm, (year), DOI: 10.1039/c3ce41215f.	
2	Please carefully check the spelling of all author names. This is important for the correct indexing and future citation of your article. No late corrections can be made.	
3	Please check that the inserted GA image and text are suitable.	
4	Although there is a discussion of ESI in the text, ESI does not appear to have been provided. Do you wish to provide ESI or would you like this citation to be removed or changed?	
5	The word "cookie" might not be understood by all readers, so this has been changed to "disk" throughout. Please check this is acceptable.	
6	Fig. 4: The EDS pattens are too small and the resolution too low to clearly see. Please provide high resolution versions (preferably 600 dpi TIF files).	
7	Please check that ref. 8a and 11d have been displayed correctly.	
8	As two versions of ref. 13e were supplied, the second version of ref. 13e has been changed to ref. 13f and all of the subsequent references renumbered accordingly. Please check that the renumbering is correct and that all of the citations within the text correspond to the correct references, and indicate any changes required.	
9	Ref. [14b]: Please provide: full list of author names (including initials).	

CrystEngComm

RSC Publishing

COMMUNICATION

Microwave-hydrothermal synthesis of single-crystalline Co_3O_4 spinel nanocubes

Cite this: DOI: 10.1039/c3ce41215f

Received 23rd June 2013,
Accepted 26th July 2013

DOI: 10.1039/c3ce41215f

www.rsc.org/crystengcomm

Tatiana A. Mulinari,[a] Felipe A. La Porta,*[ab] Juan Andrés,[b] Mário Cilense,[a] José A. Varela[a] and Elson Longo[a]

An efficient microwave-hydrothermal (MAH) method has been developed for the synthesis of highly crystalline Co_3O_4 spinel nanocubes *via* β-$Co(OH)_2$ without any surfactant assistance. The structure and surface chemical composition along the growth process are studied. The effects as well as the merits of the MAH method on the processing and characteristics of obtained Co_3O_4 spinel nanocubes are highlighted.

In recent years, the controllable synthesis of nano- or micro-sized transition metal oxides with different morphologies has attracted considerable interest because their properties depend on not only their chemical composition, but also on their structure, morphology, dimension and size distribution.[1] Among transition metal oxides, cobalt oxide (Co_3O_4) nanostructures have been investigated due to their remarkable record of widespread applications for pigments, catalysts, gas sensors, magnetic compounds, and energy storage materials.[2]

Well-defined Co_3O_4 nanostructures with various morphologies, including nanotubes, nanorods, nanowires, nanocubes, nanospheres, nanoflowers and nanosheets, have been successfully synthesized using a variety of methods.[3] However, a prerequisite for many of new applications is the availability of small size, polydisperse, and highly crystalline nanocrystals. In addition to these techniques, the preparation of Co_3O_4 *via* solution chemical routes provides a promising option for the large-scale production of this material.[4] Therefore, it is important to develop new processing material methods at low costs which are environmentally friendly and possess the possibility of the formation of materials at the micro- and nano-scale with well-defined morphologies.

Microwave-assisted chemistry is becoming very attractive in all areas of synthetic chemistry because it has advantages over other conventional methods.[5] From the pioneering work of Gedye *et al.* in 1986,[6] this method has been extensively used in organic synthesis while the research of Komarneni and Roy[7] in 1985 was the beginning of microwave-assisted inorganic syntheses. More recently, this technique has been extensively applied to the preparation of inorganic nanostructured materials with a wide range of applications.[8] Furthermore, the MAH method offers a fast, inexpensive, and highly reproducible approach for the synthesis of nanoparticles as compared with methods based on conductive heating, and different structural forms of the same compounds can be obtained with changes in the synthetic parameters, such as pH, temperature, raw material, or time.[8] In particular, Bilecka and Niederberger[9] reported the versatility of the method for the synthesis of nanoparticles while Kappe *et al.*[10] published a complete review on the subject.

The MAH method has unique characteristics associated with rapid heating and the absence of a temperature gradient as well as the enhancement of reaction rates, improved material quality and size distributions in nanomaterials.[11] Heating and driving chemical reactions by microwave energy has been an increasingly popular theme in the material synthesis. However, the mechanism associated with microwave effects in synthesis are not well understood.[9,12] In particular, different strategies to obtain Co_3O_4 nanomaterials by using the MAH method have been previously reported.[13] The present procedure described in this paper demonstrated that the MAH method combined with any surfactant-free condition leads to shorter reaction time, higher yield, a clean reaction product and easier work-up than classical thermal processing. The structure and surface chemical composition are studied along the growth process. The effects as well as the merits of the MAH method on the processing and characteristics of the Co_3O_4 spinel nanocubes obtained are highlighted.

Co_3O_4 nanocubes were synthesized by the MAH method using 1 mL of a solution of sodium hydroxide (1 mol L^{-1}) together with 3.94 mmol of cobalt nitrate in 50 mL of deionized water at 140 °C for 10–60 min. The samples were characterized by X-ray diffraction (XRD) in the 2θ range from 10° to 110° with 1° min^{-1} in the Rietveld routine (both with a step of 0.02° s^{-1}). To gain insight into the shape evolution and to unravel a formation mechanism of these distinctive Co_3O_4 nanocubes, X-ray photoelectron spectroscopy (XPS), field emission scanning electron microscopy (FE-

[a]*Instituto de Química, UNESP, PO Box 355, 14801-970, Araraquara, SP, Brazil*
[b]*Department of Physical and Analytical Chemistry, Univ Jaume I, Castelló de la Plana, 12071, Spain. E-mail: felipe_laporta@yahoo.com.br; Fax: +55 16 3301-9691; Tel: +55 16 3301-9892*

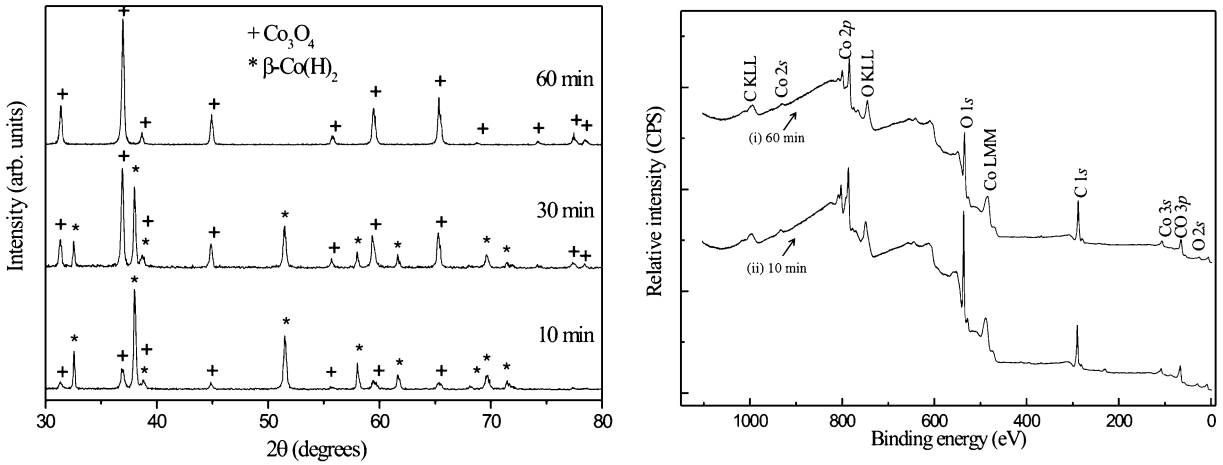

Fig. 1 (a) XRD patterns and (b) XPS survey spectrum of the β-$Co(OH)_2$ and Co_3O_4 nanoparticles processed in MAH at 140 °C for different durations.

SEM) using FEG-VP JEOL and transmission electron microscopy (TEM) have been employed.

Fig. 1(a) exhibits that XRD patterns of all diffraction peaks perfectly indexed to β-$Co(OH)_2$ and Co_3O_4 which is in agreement with the Joint Committee on Powder Diffraction Standards (JCPDS) card 30-443 and 42-1467, respectively.[14] The diffraction peaks are significantly broadened because of the very small crystallite size. The mean of size crystallites, T, was calculated from the Scherrer method (see Table 1).

The Rietveld refinement method[15] was employed with the specific objective to analyze and understand whether there are differences in the structural arrangements and to determine the percentage of the second phase in the samples processed in the MAH system (see ESI†). Table 1 shows the Rietveld refinement of the samples obtained by the MAH method. In this table, fitting parameters (R_{wp}, R_p, R_b, χ^2, and S) indicate good agreement between refined and observed XRD patterns for the samples obtained by the MAH method. The lattice parameters, unit cell volume and atomic positions were obtained from a GSAS program.[16] In this case, it was noted that the lattice parameters and unit cell volumes are very close to those published in the literature.

However, some variations in the atomic positions related to oxygen atoms were observed while cobalt atoms have fixed atomic positions. These results indicate that the position of oxygen atoms is very disturbed in the lattice. Therefore, we believe these variations in atomic positions of oxygen atoms can lead to the formation types of distortions on [O–Co–O] bonds and consequently promotes different levels of distortions on the [CoO_6] and/or [CoO_4] clusters in the lattice. Although a detailed mechanistic study goes beyond the scope of this communication, preliminary results will be briefly discussed.

Surface structure plays an important role in the properties of nanomaterials, including the reactivity, stability, solubility, melting point and electronic structure.[17] XPS measurements were performed on both types of β-$Co(OH)_2$ and Co_3O_4 nanomaterials to compare the surface purity and the degree of oxidation. Complete survey spectra of two synthesized nanomaterials are displayed in Fig. 1(b). An analysis of the results reveals that peaks of the Co 2p, O 1s and C 1s regions highlights the absence of any other metallic or inorganic species.

High-resolution XPS spectra of Co 2p and O 1s of the as-synthesized samples at 10 and 60 min are included for comparison purposes (see Fig. 2). All spectra were referenced to the aliphatic carbon at the binding energy (BE) of 285.0 eV. The composition of the surface region was determined from the ratio of relative peak areas corrected by sensitivity factors (Scofield) of corresponding elements. Spectra were fitted without placing

Table 1 Rietveld refinement results for the Co_3O_4 spinel nanocubes processed in MAH at 140 °C for different durations

	ICSD[a]		10 min		30 min		60 min	
Lattice parameter	β-$Co(OH)_2$	Co_3O_4	β-$Co(OH)_2$	Co_3O_4	β-$Co(OH)_2$	Co_3O_4	β-$Co(OH)_2$	Co_3O_4
a (Å)	3.186	8.072	3.184	8.082	3.178	8.067	—	8.089
c (Å)	4.653	—	4.662	—	4.65	—	—	
R_{wp} (%)	—		13.86		17.38		12.82	
R_p (%)	—		9.90		10.10		9.35	
R_b (%)	—		1.622		2.509		1.142	
X^2	—		1.579		2.889		1.406	
S	—		1.257		1.700		1.186	

[a] ICSD no. 88940 and 36256, respectively.[13]

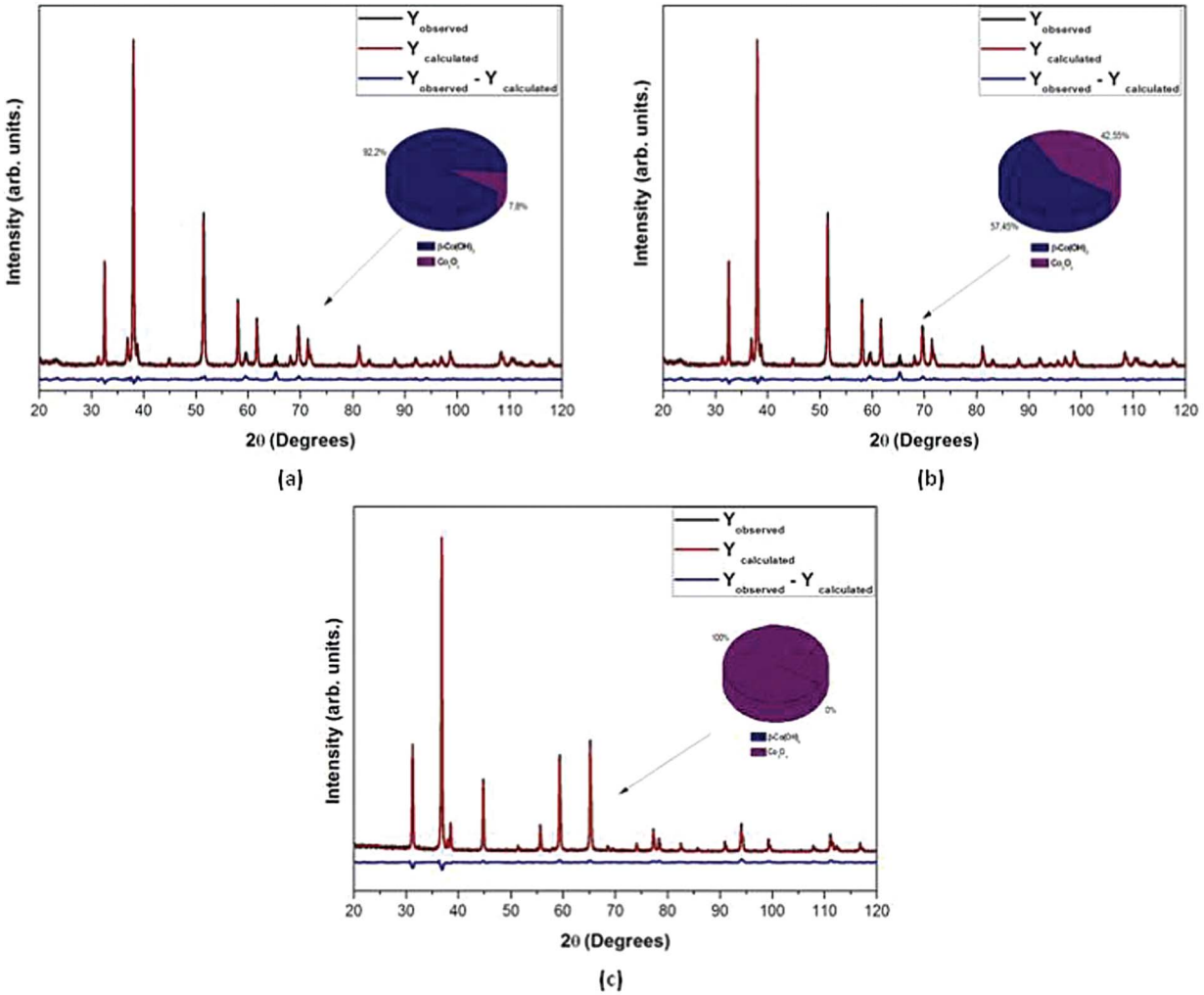

Fig. 2 Rietveld refinement plot of Co_3O_4 spinel nanocubes processed by MAH at 140 °C for different durations: (a) 10 min, (b) 30 min and (c) 60 min.

constraints using multiple Voigt profiles. Values of BE are around 532.50 eV for O 1s and 62.25 for Co 3p at 10 min and 60 min, respectively, and BE values are around 534.35 eV and 64.60 for O 1s and Co 3p, respectively. These results are consistent with BE values reported by Wagner *et al.*[18] and Yang *et al.*[19]

The high-resolution Co 2p spectrum shows a spin–orbit splitting into 2p1/2 and 2p3/2 components. BE values of Co 2p3/2 peaks at 781.15 and 779.87 eV can be associated with the surface phase of clean β-$Co(OH)_2$ and Co_3O_4 for samples at 10 and 60 min, respectively; O 1s spectra also show similar results (Fig. 3). For the sample prepared at 10 min, peaks at 529.99, 531.43 and 532.92 eV, can be assigned to oxygen species in Co_3O_4, β-$Co(OH)_2$ and H_2O molecules, respectively; for the sample at 60 min, peaks at 530.20, 531.73 and 532.92 eV can be associated to oxygen species in Co_3O_4, H_2O molecules and C=O, respectively. The contribution of NO_3^- anions to this peak should be negligible as the relative atomic concentration of N with respect to O is less than 2%. In the present case, due to the "salting-out" effect,[20] the oxygen solubility in the synthetic solution is reduced which delays the conversion of β-$Co(OH)_2$ into Co_3O_4. The intensities of shake-up satellite peaks of the Co 2p1/2 branch in the sample at 60 min are important. The spin–orbit splitting of 15.39 eV confirms the pure-phase Co_3O_4 which is in good agreement with the values reported in the literature.[21] XPS measurements have the potential to provide detailed mechanistic insight; both dissolution and redox reactions occuring continuously in MAH system has been the role key during the growth process. Thus, part of the Co^{2+} must be oxidized to obtain Co_3O_4 spinel nanocubes. The peak quantification produced a ratio of Co to O which is in excellent agreement with the stoichiometry of Co_3O_4 for 60 min of synthesis.

FE-SEM images in Fig. 4 show that both crystalline agglomerates of β-$Co(OH)_2$ and Co_3O_4 possess disk and nanocubes shapes, respectively, and it corresponds to a polydisperse sample. The systematic adjustment of reaction parameters, such as reaction time, temperature, pH, concentration, and the selection of precursors, and use or lack of surfactants can be used to control of the growth of nanoparticles by MAH synthesis to give the desired size and shape. An elemental analysis reveals that the products contain only Co and O atoms which indicates the sample purity. We believe that this aggregation process is related to the

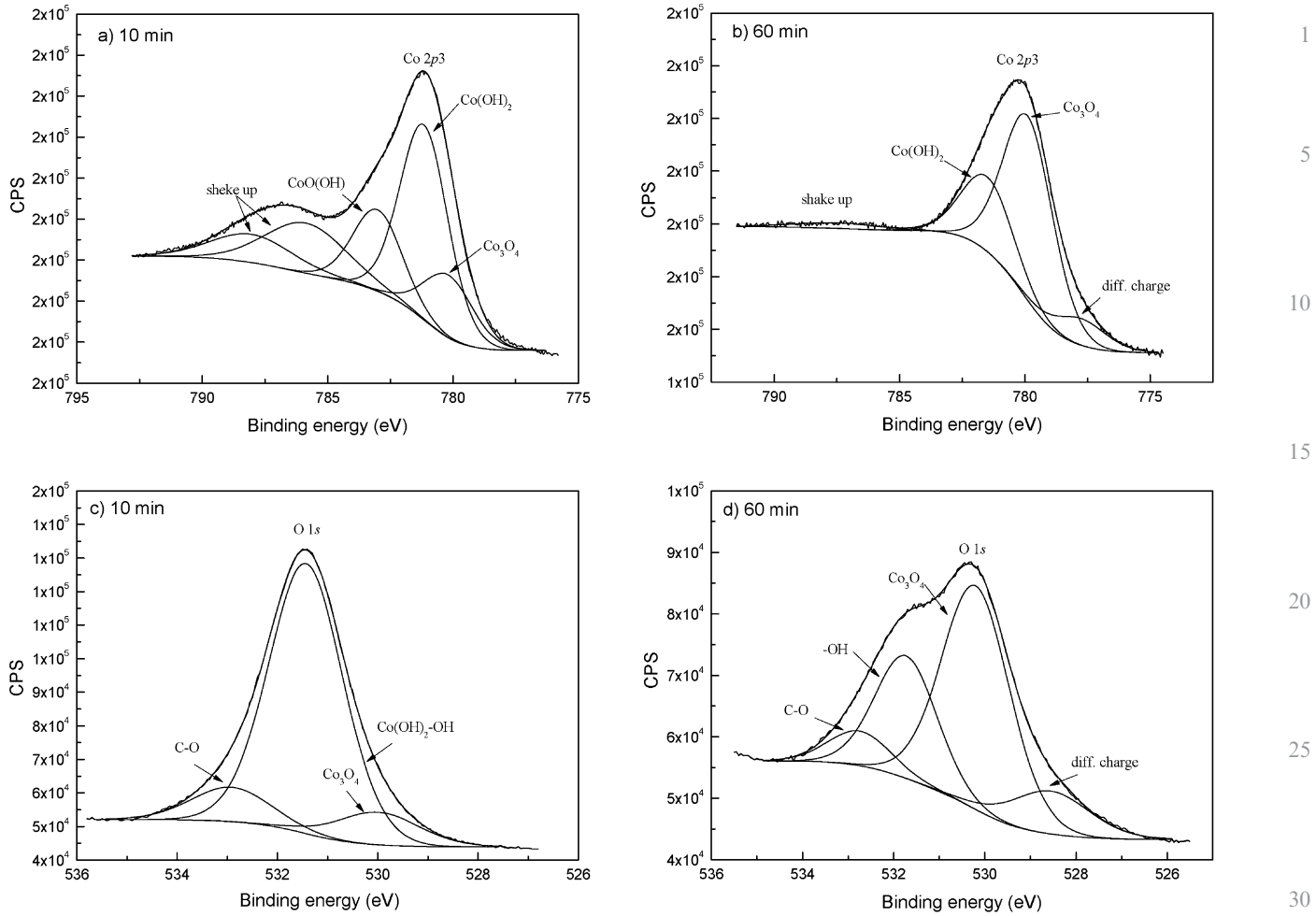

Fig. 3 Cobalt $2p_3$ oxygen 1s XPS sample spectra.

increase in effective collision rates between small particles by microwave radiation. Co_3O_4 nanocubes have been previously reported in the literature.[21]

Calculated XRD data of the formed Co_3O_4 nanocrystals are in good agreement with the observed values in our TEM images displayed in Fig. 5. No signs of a secondary phase are observed using XRD or TEM images of samples processed by the MAH method at 60 min, whereas a TEM analysis indicates the high crystallinity of the Co_3O_4 nanocubes and resulting polydisperse nanocrystals. The SAED (see Fig. 5) shows a poorly defined hexagonal spot pattern for sample at 10 min and some particles are amorphous, indicating the relatively poor single-crystallinity of these disk-like and nanocube structures and some particles exhibit a degree of amorphous nature. Thus, with the evolution of the system starting at longer durations of synthesis, we have a transformation to more pronounced β-$Co(OH)_2$ phase (disk-like) in Co_3O_4 (nanocubes) and an increase in the crystallinity of the material and the topotactic transformation to (111) planes of Co_3O_4. Furthermore, is very difficult to make isolated nanocrystals of Co_3O_4, in part because the attractive forces between the particles are large. However, the MAH method offers some advantages for nanoparticle synthesis in that nanocrystal nucleation and growth can be separated very clearly and thus polydisperse nanoparticles can be obtained and result in differently sized and shaped particles and provide superior reaction control.

The morphology and single crystalline nature of as-formed nanoparticles can be described *via* a nucleation–dissolution–recrystallization mechanism which was developed for the growth of a variety of well-defined crystals[8a] and indicates that the formation of these aggregates does not proceed *via* the classical ion-attachment mechanism but by the oriented aggregation of small primary subunits as proposed by Cölfen and co-workers.[22] Nanoparticles can undergo a self-assembly process and arrange in a highly oriented fashion and thus form mesocrystals. A large number of small nanoparticles initially originates inside a solution by nucleation and subsequent limited molecular- or ion-mediated growth. As a consequence, this mechanism involves the formation of a high concentration of aggregated nanoparticles with predominant growth controlled by the coalescence process.

On the basis of the above results, a growth mechanism of Co_3O_4 mesocrystals can be proposed involving two stages: (i)

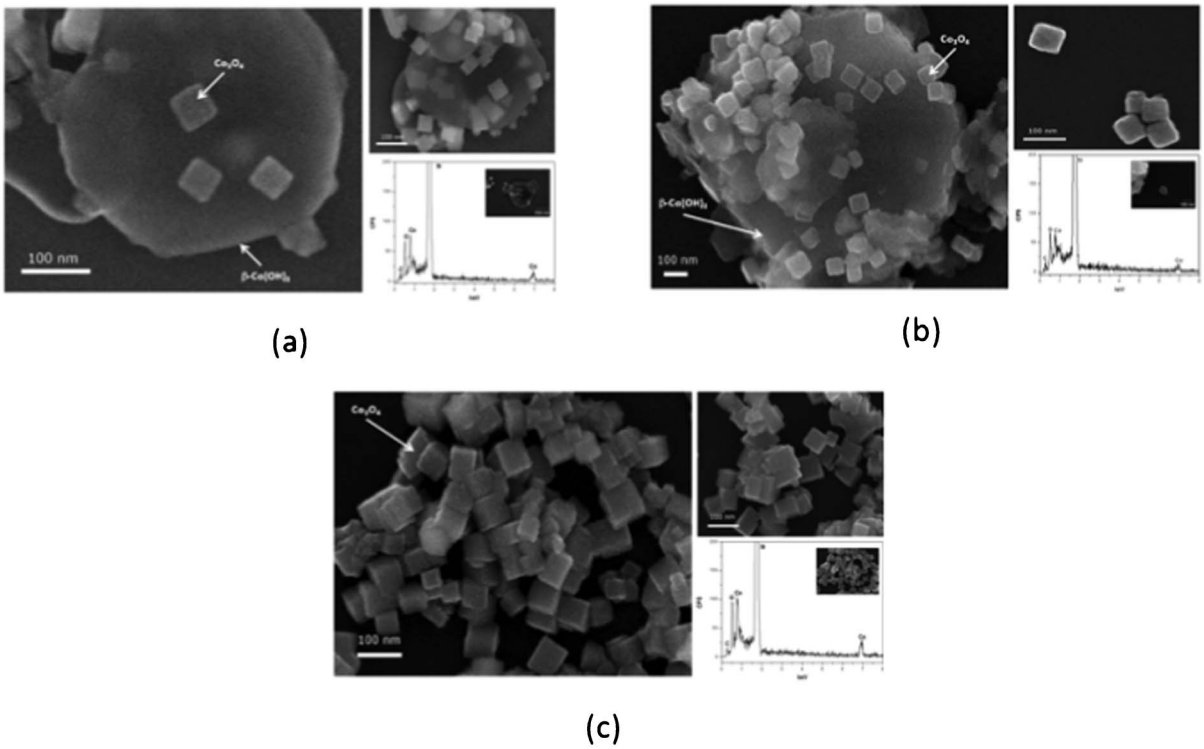

Fig. 4 FEG-SEM image and EDS patterns of samples processed by the MAH method at 140 °C for different times.

cobalt nitrate hydrolysis is the first step which provides the formation of β-$Co(OH)_2$; (ii) thereafter, fast heating to 140 °C produces homogeneous nucleation, dissolution and recrystallization processes for the structural transformation and to obtain Co_3O_4 nanocubes. Because of preferential dissolving since atoms at the edges and apex have relatively high chemical potentials,

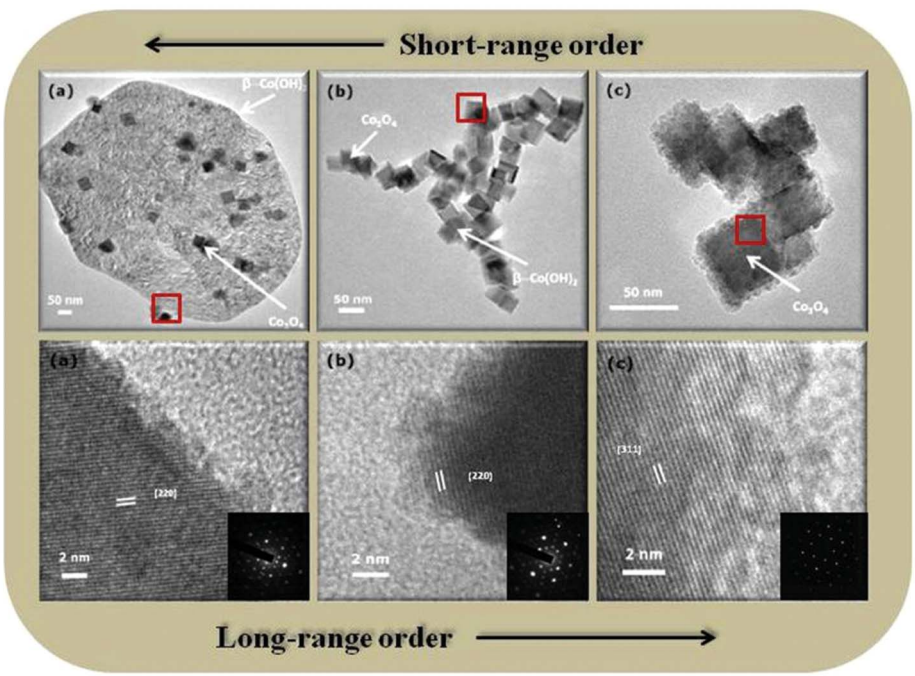

Fig. 5 TEM and HRTEM of Co_3O_4 spinel nanocubes.

some of the nanocubes are imperfect. They are formed in a self-assembly growth process that is governed by the equilibrium of repulsive and attractive interactions that makes fabrication of complex assemblies possible with great ease.

The Co_3O_4 belongs to the normal-spinel crystal structure based on a cubic close packing array of oxide ions where Co^{2+} ions occupy the tetrahedral clusters (CoO_4) and Co^{3+} ions occupy the octahedral clusters (CoO_6).[19,20] Octahedral Co^{3+} ions have a d^6 configuration at a low-spin state while tetrahedral Co^{2+} ions have a d^7 configuration with a high-spin state.[23] Raman scattering can be observed in cubic structures because the central symmetry is broken due to many factors such as oxygen vacancies, impurities, defects, strain effects and even external conditions. This effect induces polarization, and the local structure of both tetragonal and octahedral arrangements are distorted. Fig. 6 shows Raman spectra of Co_3O_4 nanocubes. Five Raman bands at 194, 429, 482, 602 and 707 cm^{-1} (A1g + Eg + 3F2g) are visible in spectra. The band at 707 cm^{-1} can be associated with the octahedral clusters (CoO_6) characteristic which is assigned to the A1g species in the Oh^7 spectroscopic symmetry.[24] Raman bands with medium intensity located at 429 and 482 cm^{-1} have Eg and $F2g^{(2)}$ symmetry, respectively, whereas the weak band located at 602 cm^{-1} has $F2g^{(1)}$ symmetry. Another band at 194 cm^{-1} corresponds to tetrahedral clusters (CoO_4), which is attributed to $F2g^{(3)}$ symmetry.[25]

In summary, a novel preparation method, based on the MAH treatment method, of highly crystalline cubic Co_3O_4 spinel nanocubes without any surfactant assistance is reported. XRD, XPS, FE-SEM and TEM measurements were employed to investigate structural, surface chemical composition as well as the growth process of synthesized nanomaterials. With this method, both the size and shape of Co_3O_4 can be controlled under "one-pot" conditions at relatively low reaction temperatures which can be extended to the preparation of other nanostructures. A possible growth mechanism for Co_3O_4 nanocubes based on a mesoscale self-assembly process is proposed. Consequently, we have developed a fast and effective procedure for the synthesis of Co_3O_4 nanomaterials for improving the application performance with reactive, stable and oriented Co_3O_4 nanocubes which have promising applications as photocatalysts, solar cells and optoelectronic devices.

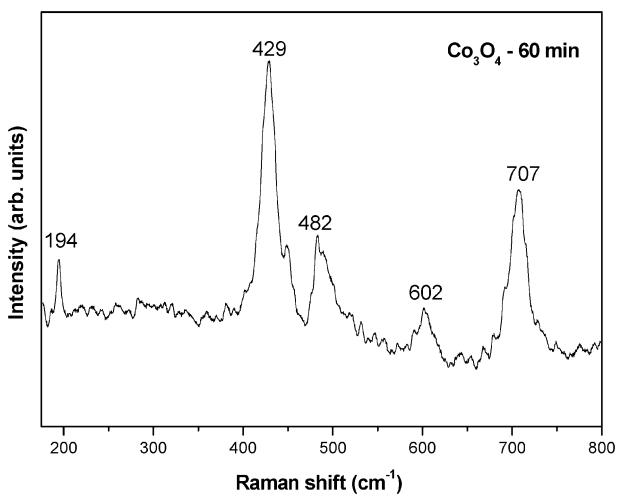

Fig. 6 Micro-Raman spectra of Co_3O_4 spinel nanocubes.

References

1 (*a*) X. Peng, L. Manna, W. Yang, J. Wickham, E. Scher, A. Kadavanich and A. P. Alivisatos, *Nature*, 2000, **404**, 59; (*b*) C. Petit, A. Taleb and M. P. Pileni, *Adv. Mater.*, 1998, **10**, 259; (*c*) J. T. Han, Y. H. Huang, X. J. Wu, C. L. Wu, W. Wei, B. Peng, W. Huang and J. B. Goodenough, *Adv. Mater.*, 2006, **18**, 2145; (*d*) J. Chen, L. N. Xu, W. Y. Li and X. L. Gou, *Adv. Mater.*, 2005, **17**, 582; (*e*) R. Yan, D. Gargas and P. Yang, *Nat. Photonics*, 2009, **3**, 569.

2 (*a*) X. Xie and W. Shen, *Nanoscale*, 2009, **1**, 50; (*b*) Y. Wang, H. Xia, L. Lu and J. Lin, *ACS Nano*, 2010, **4**, 1425; (*c*) H. X. Mai, L. D. Sun, Y. W. Zhang, R. Si, W. Feng, H. P. Zhang, H. C. Liu and C. H. Yan, *J. Phys. Chem. B*, 2005, **109**, 24380.

3 (*a*) X. Xie, Y. Li, L. Zhi-Quan, M. Haruta and W. Shen, *Nature*, 2009, **458**, 746; (*b*) J. Feng, *Chem. Mater.*, 2003, **15**, 2829; (*c*) H. Tüysüz, M. Comotti and F. Schüth, *Chem. Commun.*, 2008, 4022.

4 Z. Fei, S. He, L. Li, W. Ji and C. T. Au, *Chem. Commun.*, 2012, **48**, 853.

5 T. N. Glasnov and C. O. Kappe, *Chem.–Eur. J.*, 2011, **17**, 11956.

6 R. Gedye, F. Smith, K. Westaway, H. Ali, L. Baldisera, L. Laberge and J. Rousell, *Tetrahedron Lett.*, 1986, **27**, 279.

7 S. Komarneni and R. Roy, *Mater. Lett.*, 1985, **3**, 165.

8 (*a*) F. A. La Porta, M. M. Ferrer, Y. V. B. Santana, C. W. Raubach, V. M. Longo, J. R. Sambrano, E. Longo, J. Andrés, M. S. Li and J. A. Varela, *J. Alloys Compd.*, 2013, **556**, 153; (*b*) V. M. Longo, L. S. Cavalcante, E. C. Paris, J. C. Sczancoski, P. S. Pizani, M. S. Li, J. Andres, E. Longo and J. A. Varela, *J. Phys. Chem. C*, 2011, **115**, 5207; (*c*) H.-Q. Wang and T. Nann, *ACS Nano*, 2009, **3**, 3804; (*d*) H. Katsuki and S. Komarneni, *J. Ceram. Soc. Jpn.*, 2011, **119**, 525; (*e*) Y. V. B. Santana, C. W. Raubach, M. M. Ferrer, F. La Porta, J. R. Sambrano, V. M. Longo, E. R. Leite and E. Longo, *J. Appl. Phys.*, 2011, **110**, 123507.

9 I. Bilecka and M. Niederberger, *Nanoscale*, 2010, **2**, 1358.

10 M. Baghbanzadeh, L. Carbone, P. D. Cozzoli and C. O. Kappe, *Angew. Chem., Int. Ed.*, 2011, **50**, 11312.

11 (*a*) D. P. Volanti, M. O. Orlandi, J. Andrés and E. Longo, *CrystEngComm*, 2010, **12**, 1696; (*b*) L. R. Macario, M. L. Moreira, J. Andrés and E. Longo, *CrystEngComm*, 2010, **12**, 3612; (*c*) L. F. da Silva, W. Avansi Jr, M. L. Moreira, J. Andrés, E. Longo and V. R. Mastelaro, *CrystEngComm*, 2012, **14**, 4068; (*d*) L. S. Cavalcante, V. M. Longo, J. C. Sczancoski, M. A. P. Almeida, A. A. Batista, J. A. Varela, M. O. Orlandi, E. Longo and M. S. Li, *CrystEngComm*, 2012, **14**, 853.

12 (*a*) G. B. Dudley, A. E. Stiegman and M. R. Rosana, *Angew. Chem., Int. Ed.*, 2013, **52**, 7918; (*b*) L. Pan, X. Liu, Z. Sun and C. Q. Sun, *J. Mater. Chem. A*, 2013, **1**, 8299; (*c*) C. O. Kappe, B. Pieber and D. Dallinger, *Angew. Chem., Int. Ed.*, 2013, **52**, 1088 and references there in.

13 (*a*) C. Sun, X. Su, F. Xiao, C. Niu and J. Wang, *Sens. Actuators, B*, 2011, **157**, 681; (*b*) Q. S. Chen and Y. Wang, *J. Mater. Chem.*, 2010, **20**, 9735; (*c*) P. Zhang, G. X. Hu, S. J. Bao, J. Guo, C. Lei, C. J. Cai, D. Z. Jia and R. Y. Wang, *Mater. Lett.*, 2012, **83**, 195; (*d*) S. K. Meher and G. R. Rao, *J. Phys. Chem. C*, 2011, **115**, 25543; (*e*) L. Y. Man, B. Niu, H. Y. Xu, B. Q. Cao and J. Q. Wang, *Mater.*

Res. Bull., 2011, **46**, 1097; (*f*) J. Q. Wang, B. Niu, G. D. Du, R. Zeng, Z. X. Chen, Z. P. Guo and S. X. Dou, *Mater. Chem. Phys.*, 2011, **126**, 747; (*g*) J. Yan, T. Wei, W. M. Qiao, B. Shao, Q. K. Zhao, L. J. Zhang and Z. J. Fan, *Electrochim. Acta*, 2010, **55**, 6973.

14 (*a*) K. Martin and G. McCarthy, *ICDD Grant-in-Aid*, North Dakota State University, Fargo, North Dakota, USA, 1990; (*b*) *Natl. Bur. Stand., Monogr. (U. S.)*, 1978, 25(15), 29.

15 H. M. Rietveld, *J. Appl. Crystallogr.*, 1969, **2**, 65.

16 A. C. Larson and R. B. Von Dreele, General Structure Analysis System (GSAS), *Los Alamos National Laboratory Report LAUR*, 1994, vol. 86, p. 748.

17 A. P. Alivisatos, *J. Phys. Chem.*, 1996, **100**, 13226.

18 C. D. Wagner, W. W. Riggs, L. E. Davis, J. F. Moulder and G. E. Muilenberg, *Handbook of X-ray Photoelectron Spectroscopy*, Physical Electronics Division, Perkin-Elmer Corporation, Wellesley, MA, 1979.

19 J. Yang, H. Liu, W. N. Martens and R. L. Frost, *J. Phys. Chem. C*, 2010, **114**, 111.

20 J. Feng and H. C. Zeng, *Chem. Mater.*, 2003, **15**, 2829.

21 R. Xu and H. C. Zeng, *Langmuir*, 2004, **20**, 9780.

22 (*a*) H. Cölfen and M. Antonietti, *Angew. Chem., Int. Ed.*, 2005, **44**, 5576; (*b*) R.-Q. Song and H. Cölfen, *Adv. Mater.*, 2010, **22**, 1301; (*c*) F. C. Meldrum and H. Cölfen, *Chem. Rev.*, 2008, **108**, 4332; (*d*) H. Cölfen and M. Antonietti, *Mesocrystals and Nonclassical Crystallization.*, John Wiley & Sons Ltd, Chichester, UK, 2008; (*e*) L. Zhou and P. O'Brien, *J. Phys. Chem. Lett.*, 2012, **3**, 620.

23 S. K. Tripathy, M. Christy, N.-H. Park, E.-K. Suh, S. Anand and Y.-T. Yu, *Mater. Lett.*, 2008, **62**, 1006.

24 (*a*) D. Gallant, M. Pezolet and S. Simard, *J. Phys. Chem. B*, 2006, **110**, 6871; (*b*) V. G. Hadjiev, M. N. Iliev and I. V. Vergilov, *J. Phys. C: Solid State Phys.*, 1988, **21**, L199.

25 S. G. Kwon, Y. Piao, J. Park, S. Angappane, Y. Jo, N.-M. Hwang, J.-G. Park and T. Hyeon, *J. Am. Chem. Soc.*, 2007, **129**, 12571.